

# Assessment of corneal and lens clarity in children with Wilson disease



Sibel Doğuizi, MD,<sup>a</sup> Serdar Özateş, MD,<sup>b</sup> Ferda Özbay Hoşnut, MD,<sup>c</sup> Gülseren Evirgen Şahin, MD,<sup>c</sup> Mehmet Ali Şekeroğlu, MD,<sup>a</sup> and Pelin Yılmazbaş, MD<sup>a</sup>

---

<b>PURPOSE</b>	To investigate the effect of copper accumulation on corneal and lens clarity in children with Wilson disease (WD) compared to healthy children.
<b>METHODS</b>	This multicenter cross-sectional study included 24 subjects with WD and 25 age-matched controls. Clinical and laboratory characteristics of the WD subjects were recorded. The Pentacam HR imaging system was used both for lens densitometry and corneal densitometry.
<b>RESULTS</b>	Corneal densitometry values were higher in the posterior 6-10 mm ( $P = 0.021$ ), posterior 10-12 mm ( $P < 0.001$ ), posterior total diameter ( $P = 0.037$ ), total thickness 10-12 mm ( $P = 0.032$ ), and total thickness 6-10 mm zones and layers ( $P = 0.040$ ) in the WD eyes than in control eyes. The lens densitometry values of zone 1 were higher in WD eyes ( $P < 0.001$ ). There was a significant relationship between corneal densitometry values in the posterior 10-12 mm zones ( $P = 0.012$ ; $r = 0.527$ ) and the duration of WD and liver copper content ( $P = 0.016$ ; $r = 0.507$ ). A statistically significant correlation was also detected between lens densitometry values in zone 1 and WD duration ( $P = 0.018$ ; $r = 0.426$ ).
<b>CONCLUSION</b>	In this study cohort, children with WD had decreased corneal and lens clarity even in cases without Kayser-Fleischer rings and sunflower cataracts. Densitometry measurements using Scheimpflug imaging provided detection of corneal and lens involvement in the early stages of WD. (J AAPOS 2019;23:147.e1-8)

---

Wilson disease (WD) is a rare, autosomal recessive disorder of hepatic copper metabolism characterized by copper accumulation in hepatocytes and in extrahepatic tissue, including the brain, lens, and cornea. Hepatocytes express the *ATP7B* gene, and its protein product is copper-transporting adenosine triphosphatase (ATPase).<sup>1,2</sup> Mutations of the *ATP7B* gene, which is localized in chromosome 13 (13q14.3), result in defective *ATP7B* function and thus the impaired biliary excretion of copper.<sup>1,2</sup> Copper accumulates in the liver, brain, cornea, lens, and other organs, resulting in hepatic, neurological/psychiatric, and ocular symptoms.<sup>3</sup> In children, unlike in adults, disease onset is primarily hepatic. Younger age groups in their first and second decades of life commonly present hepatic symptoms, whereas

neurologic and psychiatric manifestations occur mostly in the third decade.<sup>4</sup>

WD is characterized by different ophthalmological manifestations. Kayser-Fleischer (KF) corneal rings, caused by the granular deposition of copper in the Descemet's membrane, are considered to be the hallmark of WD. They appear as a granular golden-greenish layer near the limbus<sup>4</sup> and are best detected on slit-lamp examination. Although the occurrence of KF rings in children with liver disease is variable and reportedly uncommon, the rings may be seen in up to 80%-98% of adult patients, especially with neurological and psychiatric presentation.<sup>4,5</sup> Sunflower cataracts, although rare, are also characteristic of WD, indicating copper deposits in the middle of the lens.<sup>2</sup> They too are best found on slit-lamp examination.<sup>6</sup> Other, rare ophthalmological manifestations of WD include night blindness, exotropic strabismus, optic neuritis, and optic disk pallor.<sup>4,5</sup>

WD diagnosis is especially challenging in children, because the clinical presentations range from asymptomatic liver disease to cirrhosis or acute liver failure. Neurologic and psychiatric symptoms are rarely seen.<sup>5</sup> KF rings and sunflower cataracts, when present, are distinctive and valuable diagnostic signs. They are not usually observed on slit-lamp examination of pediatric WD patients with liver disease; KF rings are usually present when there is neurologic involvement.<sup>7</sup> Sunflower cataracts are also very rare in children.<sup>8</sup> It should be

Author affiliations: <sup>a</sup>Department of Ophthalmology, Ulucanlar Eye Training and Research Hospital, Ankara, Turkey; Departments of <sup>b</sup>Ophthalmology and <sup>c</sup>Pediatric Gastroenterology, Dr. Sami Ulus Children's Health and Disease Training and Research Hospital, Ankara, Turkey

Submitted August 1, 2018.

Revision accepted December 27, 2018.

Published online May 9, 2019.

Correspondence: Dr. Sibel Doğuizi, MD, Department of Ophthalmology, Ulucanlar Eye Training and Research Hospital, Altındag, 06230, Ankara, Turkey (email: [eryigits@yaboo.com](mailto:eryigits@yaboo.com)).

Copyright © 2019, American Association for Pediatric Ophthalmology and Strabismus. Published by Elsevier Inc. All rights reserved.

1091-8531/\$36.00

<https://doi.org/10.1016/j.jaaapos.2018.12.010>

emphasized that the nondetection of KF rings and sunflower cataracts in the slit-lamp examination does not necessarily mean that the lens and cornea are unaffected by copper accumulation.

The Pentacam HR (Oculus Optikgeräte, GmbH, Wetzlar, Germany) is a noninvasive optical system that uses a rotating Scheimpflug camera to produce anterior and posterior corneal topographic maps, corneal pachymetry, and three-dimensional analysis of the anterior chamber.<sup>9,10</sup> The system can also be used to obtain precise and reproducible corneal and lens densitometry data in different ocular and systemic diseases and to quantitatively measure corneal and lens opacity.<sup>11,12</sup> The aim of the current study was to investigate the effect of copper accumulation on corneal and lens clarity in children with WD using the Pentacam HR.

## Subjects and Methods

This prospective, cross-sectional comparative study was approved by the Ethics Committee of Numune Eye Training and Research Hospital and was conducted in accordance with the principles of the Declaration of Helsinki. Written informed consent was obtained from the parents or legal guardians of the subjects prior to enrollment. Both pediatric WD subjects and age- and sex-matched controls were recruited from January to November 2017 at Ulucanlar Eye Training and Research Hospital and at the pediatric gastroenterology clinic at Dr. Sami Ulus Children's Health and Disease Training and Research Hospital.

The WD diagnosis was based on international diagnostic criteria with regard to copper metabolism and liver biopsy, as described previously.<sup>4,13</sup> Inclusion criteria were as follows: an established diagnosis of WD (with a score  $\geq 4$ , according to the diagnostic scoring system for WD), a best-corrected visual acuity of  $\geq 20/20$  (Snellen chart), no ocular problems other than spherical or cylindrical refractive error of  $< 1.50$  D, and no other systemic disease. Additionally, only subjects with good Pentacam image quality (registering as "OK" on the instrument's examination quality specification) were included. The following were cause for exclusion: presence of a KF ring or a sunflower cataract, ocular media opacities, strabismus, nystagmus, keratoconus and corneal dystrophies, histories of uveitis or trauma, neurological disease or other diseases of the visual pathways, glaucoma, ocular surgery or injury, contact lens use, dry eye diseases, metabolic disease, or any other systemic disease that might affect the cornea and lens. Patients using chronic topical medications were also excluded.

Two ophthalmologists (SD, SO) performed a full anterior segment examination of the corneas to assess the presence of copper depositions in the Descemet's membrane and KF rings using slit-lamp biomicroscopy and Goldmann's three-mirror contact lens. All enrolled subjects underwent noncontact tonometry, dilated fundus examination, and Scheimpflug anterior segment analysis using the Pentacam HR. One eye of each subject was randomly selected for inclusion.

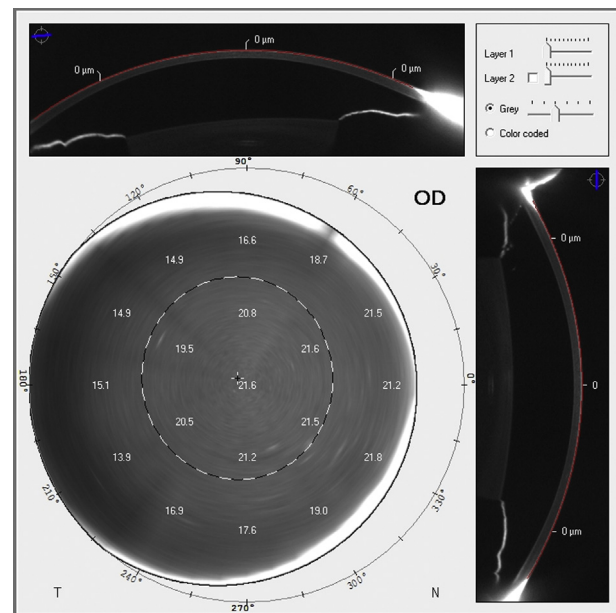


**FIG 1.** Pentacam HR-Scheimpflug image with corneal densitometry analysis of a patient with Wilson disease (WD) without Kayser-Fleischer ring. The program automatically determines the corneal apex and analyzes an area around it with a diameter of 12 mm. This area is subdivided into four concentric radial zones (0-2 mm, 2-6 mm, 6-10 mm, 10-12 mm). The output is also subdivided based on corneal depth into the anterior, central, and posterior layers. Depending on the degree of light scatter, the program quantifies the density of the cornea on a 0-100 grayscale units scale.

## Lensitometry

Backward light scattering was measured using Scheimpflug tomography to evaluate changes in corneal and lens transparency. The camera captures 25 single-slit images in  $< 2$  seconds while rotating around the eye from  $0^\circ$  to  $180^\circ$ . All measurements were performed by the same experienced masked operator in the same room under standard dim-light conditions at the same time of the day. Three measurements were taken per eye to ensure one good-quality Scheimpflug image, and the best-aligned and fixated image was included in the data analysis. We performed two consecutive measurements on each patient: the first without pupil dilation for corneal densitometric evaluation and the second after pupillary dilation for optimal screening of the whole lens. Two drops of cyclopentolate hydrochloride 1% were instilled 5 minutes apart to induce pupil dilation. The second measurements were taken approximately 45 minutes after the last drop.

Corneal densitometry values were obtained according to the previously published method.<sup>12</sup> The program automatically locates the corneal apex and analyzes the area around the apex in a diameter of 12 mm.<sup>12,14</sup> Depending on the degree of light scatter, the Pentacam HR quantifies the density of the cornea on a scale of 0-100 grayscale units (GSU), with 0 indicating no light scatter or no corneal haze and 100 indicating totally opaque corneas. A local densitometric analysis was performed by dividing the 12 mm diameter area into 4 concentric radial zones, available as software presets. The central zone, centered

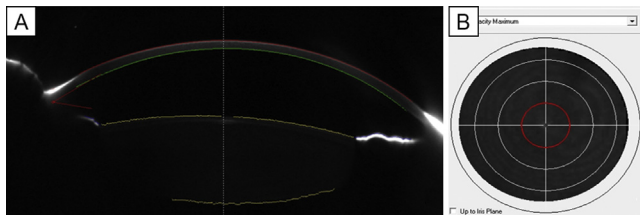


**FIG 2.** Pentacam HR-Scheimpflug image (A) with lens densitometry analysis (B) of a patient with WD without sunflower cataract.

on the apex, has a diameter of 2 mm. The second zone is an annulus from 2 mm to 6 mm in diameter. The annulus at the third zone extends from 6 mm to 10 mm, and the final extends from 10 mm to 12 mm. The output is preferably subdivided based on corneal depth into the anterior (the anterior 120  $\mu\text{m}$ ), central, and posterior (the most posterior 60  $\mu\text{m}$ ) layers (Figure 1).

The densitometry of the lens was measured using 3D scan modes. The Pentacam densitometry software evaluates the lens's volume and density by analyzing a 12 mm diameter area within the corneal apex using backward scatter mechanisms. The mean value was calculated in predefined 3D zones centered around the pupil center, where zone 1 was 2.0 mm, zone 2 was 4.0 mm, and zone 3 was 6.0 mm in diameter (Figure 2).

### Statistical Analysis

A post hoc power analysis for the differences between the posterior 10-12 mm corneal densitometry zones, and average lens densitometry values were calculated based on study results. Power levels were 84% and 98.4%, respectively. PASS 11 (Power and sample size, version 11) was used for the power analysis. Statistical analysis was performed using the Statistical Package for Social Sciences (SPSS), version 22.0 for Windows (SPSS Inc, Chicago, IL). Data were expressed as the means with standard deviations, frequency distributions, and percentages, where appropriate. The Pearson  $\chi^2$  test was used for the comparison of categorical variables. The distribution pattern of the variables was tested by visual (histogram and probability graphs) and analytical (Kolmogorov-Smirnov/Shapiro-Wilk test) tools. Normally distributed numerical data were obtained from the WD and the control groups. For the normally distributed data, the  $t$  test was used; for nonnormally distributed data, the Mann-Whitney  $U$  test. The correlations between the duration of WD and the densitometric results were tested by Pearson correlation tests. The statistical significance was set at  $P < 0.05$ .

### Results

Overall, 24 of 40 consecutive WD patients were included. The study included 49 eyes of 49 subjects, 24 of which had WD and 25 of which were the controls. The mean age of the WD subjects was  $13.4 \pm 3.8$  years (range, 6-17); of controls,  $13.3 \pm 3.0$  years (range, 7-17). There were no statistically significant differences in the age, sex, and spherical equivalent values between the two groups (Table 1).

Concerning the WD group, the mean duration of the disease was  $4.8 \pm 3.4$  years (range, 1-13). The mean level of serum ceruloplasmin was  $12.6 \pm 6.7$  mg/dl (range, 5-35 mg/dl); of 24-hour urinary copper excretion,  $308.2 \pm 200.7$   $\mu\text{g}$  (range, 38-677  $\mu\text{g}$ ); and of liver copper content,  $296.5 \pm 176.3$   $\mu\text{g/g}$  (range, 102-975  $\mu\text{g/g}$ ). See Table 2. Twelve WD patients were taking D penicillamine therapy, 8 were on D penicillamine combined with zinc salts, and 4 were taking trientine.

Corneal densitometry values are shown in Table 3. In both WD subjects and controls, the corneal densitometry values were highest in the anterior layer and lowest in the posterior. The total densitometry values were highest in the 10-12 mm zone, followed by the 0-2 mm, 2-6 mm, and 6-10 mm zones. In WD eyes, the corneal densitometry values were higher in the posterior 6-10 mm ( $P = 0.021$ ), posterior 10-12 mm ( $P < 0.001$ ), posterior total diameter ( $P = 0.037$ ), total thickness 10-12 mm ( $P = 0.032$ ), and total thickness 6-10 mm zones and layers ( $P = 0.040$ ) than in control eyes. However, there was no statistical difference in the corneal densitometry values of the other concentric zones and layers between WD patients and controls ( $P > 0.05$ ).

There was a statistically significant difference in the mean values of the average and maximum lens densitometry values of the WD and control groups ( $P < 0.001$ ,  $P = 0.006$ , resp.; Table 4). The lens densitometry values of zone 1 were significantly higher in the WD group ( $P < 0.001$ ). No statistically significant difference was found between the groups in the lens densitometry values of zone 2 and zone 3, despite the high values in WD patients ( $P = 0.084$ ,  $P = 0.075$ , resp.).

There were only statistically significant correlations between the corneal densitometry values in the posterior 10-12 mm zone ( $P = 0.012$ ;  $r = 0.527$ ) and the duration of WD and liver copper content ( $P = 0.016$ ;  $r = 0.507$ ; see Table 5).

The only statistically significant correlation was between the lens densitometry values in zone 1 and the duration of WD ( $P = 0.018$ ;  $r = 0.426$ ; see Table 6).

### Discussion

Hepatic presentation is common in most cases of pediatric WD. Diagnosing WD in young children with mild liver disease is often challenging, because these children may have normal ceruloplasmin levels and urinary copper excretion, rarely present neurological signs, and have no KF rings.<sup>4,5</sup> Furthermore, the incidence of KF rings is low in children presenting with liver disease, and sunflower cataract is extremely rare.<sup>15</sup> We investigated the effect of copper deposition on corneal and lens clarity in children with WD and the possible contribution of densitometry measurements to the assessment of the corneal and lens involvement. To our knowledge, this is the first study evaluating cornea and lens densitometry in pediatric WD.

Table 1. Demographics and clinical characteristics of Wilson disease (WD) and control subjects

Characteristic	WD group (n = 24)	Control group (n = 25)	P value
Age, years, mean $\pm$ SD (min-max)	13.4 $\pm$ 3.8 (6-17)	13.3 $\pm$ 3.0 (7-17)	0.161 <sup>a</sup>
Sex, n (%)			
Male	14 (58.3)	15 (62.5)	0.826 <sup>b</sup>
Female	10 (41.7)	10 (37.5)	
SE, mean $\pm$ SD (min-max)	0.63 $\pm$ 0.37 (0.25-2.00)	0.62 $\pm$ 0.38 (0.25-2.00)	0.837 <sup>a</sup>

SD, standard deviation; SE, spherical equivalent.

<sup>a</sup>Mann-Whitney *U* test.

<sup>b</sup> $\chi^2$  test.

Table 2. Characteristics of 24 children with Wilson disease

Patient	Age, years	Sex	Duration of WD, years	Serum Cp, mg/dl	Urinary copper excretion, $\mu$ g/24-hour	KF	Liver copper content, $\mu$ g/g	Genetic analysis	ALT	AST	GGT
1	17	F	6	10	387	Absent	471	—	241	197	37
2	13	M	5	8	541	Absent	254	—	153	144	29
3	12	F	1	16	187.7	Absent	364	—	1007	1008	42
4	16	M	6	11	244	Absent	289	—	122	109	32
5	10	M	9	7	437	Absent	301	—	40	41	41
6	16	F	7	12	83.3	Absent	276	—	47	53	31
7	8	F	5	5	324	Absent	312	—	48	59	38
8	17	M	2	13	537	Absent	291	—	92	83	45
9	17	M	12	5	265	Absent	275	ATP7B	81	48	21
10	17	M	13	7	624	Absent	115	—	68	44	68
11	12	M	5	13	500.4	Absent	102	ATP7B	241	111	110
12	15	F	6	9	405	Absent	213	—	64	62	24
13	18	F	6	14	122	Absent	282	—	128	87	19
14	8	M	1	9	295	Absent	975	ATP7B	107	71	45
15	15	F	1	14	38	Absent	157	ATP7B	72	62	31
16	9	F	1	24	44.1	Absent	334	—	242	276	363
17	11	M	4	18	97	Absent	315	—	287	241	44
18	6	M	2	35	180	Absent	388	—	52	49	35
19	10	M	2	11	677	Absent	292	ATP7B	331	202	61
20	16	M	6	9	546	Absent	118	—	74	89	27
21	15	M	4	13	80	Absent	179	ATP7B	124	117	51
22	18	M	2	18	448	Absent	263	—	134	121	18
23	14	F	4	12	165	Absent	312	—	111	78	31
24	12	F	6	11	170	Absent	240	—	101	98	33

ALT, alanine aminotransferase; AST, aspartate aminotransferase; Cp, ceruloplasmin; GGT, gamma-glutamyl transferase; KF, Kayser-Fleischer ring.

Clinical methods for examining KF rings include direct ophthalmoscopy, gonioscopy, and slit-lamp examination of the cornea. Detection of KF rings by slit-lamp examination requires the experience of the clinician, and the verification of the KF ring presence may be difficult, especially in early phases of the disease. Belkin and colleagues<sup>16</sup> introduced X-ray excitation spectrometry to objectively and sensitively determine the presence of copper ion deposits in the cornea of WD patients, aiming to overcome the poor sensitivity of slit-lamp examination. However, spectrometry has not been a routine part of current clinical practice for WD diagnosis. Ceresara and colleagues<sup>17</sup> investigated KF rings by confocal microscopy and slit-lamp biomicroscopy. Corneal copper deposits were detectable in the peripheral cornea in 75% of their WD cases using confocal microscopy, whereas these deposits were only detectable in 25% of WD cases on slit-lamp examination.<sup>17</sup> They suggested that confocal microscopy

may provide important information, particularly for suspicious WD cases. On the other hand, confocal microscopy is not widely used in clinical practice because it is difficult to perform.

Anterior segment optical coherence tomography (AS-OCT) is an alternative method of evaluating KF rings. Sridhar and colleagues<sup>18</sup> reported on 7 patients with KF rings that could have been easily measured using the AS-OCT grayscale. They also suggested that AS-OCT could be useful for assessing KF ring density and for differentiating it from copper deposits associated with other clinical conditions. Similarly, Telinius and colleagues<sup>19</sup> reported on 11 WD patients with KF rings and significantly higher subendothelial signals on Scheimpflug imaging. They suggested that Scheimpflug imaging could be an important tool for ophthalmologists with little experience in patients with WD. All these studies included only adult patients with WD and KF rings.

Table 3. Comparison of corneal densitometry measurements (grayscale units) in the Wilson disease (WD) and control groups

	WD group (n = 24), mean ± SD (min-max)	Control group (n = 25), mean ± SD (min-max)	P value <sup>a</sup>
Anterior 120 μm			
0–2 mm	16.7 ± 1.28 (14.4-19.4)	16.9 ± 1.37 (15-19.4)	0.748
2–6 mm	14.8 ± 1.3 (12.1-17.2)	15.1 ± 1.27 (13.4-17.7)	0.851
6–10 mm	14.2 ± 3.4 (10.4-27.8)	15.9 ± 4.5 (11.7-25.3)	0.326
10–12 mm	24.3 ± 8.78 (9.6-39.9)	21.7 ± 6.64 (14.9-36.6)	0.453
Total diameter	16.5 ± 2.41 (12.3-23.5)	16.7 ± 2.78 (13.9-23.3)	0.574
Center			
0–2 mm	11.1 ± 0.62 (10-12.5)	10.8 ± 0.37 (10.1-11.7)	0.603
2–6 mm	10.1 ± 0.8 (8.8-12.6)	10.0 ± 0.4 (9.3-10.6)	0.460
6–10 mm	9.7 ± 2.7 (7.9-21.2)	10.1 ± 2.3 (8.2-19.2)	0.132
10–12 mm	14.3 ± 5.1 (8.2-29.1)	12.9 ± 2.6 (9.5-19.8)	0.545
Total diameter	10.6 ± 1.8 (9.0-17.9)	10.7 ± 1.6 (9.8-17.4)	0.947
Posterior 60 μm			
0–2 mm	8.3 ± 0.7 (6.8-9.3)	8.0 ± 0.6 (6.8-9.2)	0.093 <sup>b</sup>
2–6 mm	7.9 ± 0.8 (6.4-9.6)	7.5 ± 0.5 (6.4-8.6)	0.129 <sup>b</sup>
6–10 mm	8.5 ± 2.5 (6.7-17.2)	7.4 ± 0.7 (6.6-8.6)	0.021
10–12 mm	11.4 ± 3.7 (7.6-23.3)	8.1 ± 1.1 (7.1-11.2)	<0.001 <sup>b</sup>
Total diameter	8.6 ± 1.6 (7.1-14.1)	7.7 ± 0.9 (7.1-11.1)	0.037
Total thickness			
0–2 mm	11.9 ± 0.7 (10.8-13.5)	11.6 ± 0.6 (10.1-2.8)	0.374 <sup>b</sup>
2–6 mm	10.8 ± 0.8 (9.4-12.8)	10.6 ± 0.5 (9.7-11.9)	0.974 <sup>b</sup>
6–10 mm	12.7 ± 2.8 (7.5-22.1)	10.7 ± 2.2 (8.3-15.4)	0.032
10–12 mm	16.7 ± 5.5 (8.6-30.5)	13.7 ± 3.0 (10.8-20.1)	0.040
Total diameter	11.9 ± 1.8 (9.7-18.5)	11.8 ± 1.3 (10.3-14.6)	0.877

SD, standard deviation.

<sup>a</sup>Mann-Whitney *U* test.

<sup>b</sup>*t* test.

Table 4. Comparison of the lens densitometry measurements and lens thicknesses in both groups

	Wilson (n = 24) mean ± SD (min-max)	Control (n = 25) mean ± SD (min-max)	P value <sup>a</sup>
Zone 1	8.3 ± 0.6 (7.5-10.5)	7.5 ± 0.3 (7.3-8.3)	<0.001
Zone 2	8.0 ± 0.5 (7.3-9.2)	7.8 ± 0.3 (7.3-8.9)	0.084
Zone 3	7.8 ± 0.3 (7.1-8.3)	7.7 ± 0.3 (7.1-8.2)	0.075 <sup>b</sup>
Average	8.3 ± 0.6 (7.3-9.6)	7.6 ± 0.3 (7.2-8.3)	<0.001 <sup>b</sup>
SD	1.4 ± 0.1 (0.4-2.9)	1.3 ± 0.2 (0.7-1.5)	0.051
Maximum	17.3 ± 5.7 (9.0-28.0)	13.1 ± 2.9 (10.2-22.0)	0.006
Lens thickness, mm	3.7 ± 0.3 (3.2-4.3)	3.5 ± 0.3 (3.1-4.1)	0.136 <sup>b</sup>

SD, standard deviation.

<sup>a</sup>Mann-Whitney *U* test.

<sup>b</sup>*t* test.

Our study used Scheimpflug imaging to acquire corneal densitometry values. Our results primarily showed that the values in the posterior layer and the 6-10 mm and 10-12 mm zones were higher in children with WD without KF rings than in the control group. We suggest that until the KF ring can be detected by a slit-lamp examination, copper accumulation alters the density of the peripheral and posterior layers of cornea.

Electron microscopy studies have identified copper bound to a sulfur-containing moiety in electron-dense granules seen throughout the cornea in WD patients. It is usually observed in the corneal periphery, and these peripheral hyperreflective granules lie mainly in the Descemet's membrane close to the endothelium.<sup>20</sup> These pathological findings are consistent with our results, in

which only the densitometry values of the posterior and peripheral layers were higher than the control group.

We also investigated the correlation between corneal densitometry values and clinical and laboratory findings. We found correlations only between liver copper values, duration of WD disease, and the posterior 10-12 mm zone densitometry values. Liver copper and duration of WD disease are both signs of the severity and duration of the tissue's copper exposure. These results suggest that with increasing copper deposition in the cornea, densitometry levels increase.

Sunflower cataracts, though relatively rare, are a characteristic of WD, especially in the more advanced stages of the disease.<sup>6</sup> They are caused by reversible copper deposition under the anterior capsule of the lens; hence,

Table 5. Relationship between the clinical and laboratory findings and corneal densitometry values of patients with WD

	Age	Duration of WD	Serum Cp	24-hour urinary copper excretion	Liver copper content	ALT	AST	GGT
Anterior 120 $\mu\text{m}$								
0–2 mm								
<i>r</i>	0.396	0.236	0.050	0.159	0.006	0.081	–0.043	0.108
<i>P</i>	0.068	0.290	0.825	0.480	0.978	0.722	0.849	0.631
2–6 mm								
<i>r</i>	0.379	0.300	0.015	0.157	0.054	0.034	–0.077	0.113
<i>P</i>	0.082	0.175	0.947	0.486	0.812	0.881	0.732	0.615
6–10 mm								
<i>r</i>	0.080	–0.007	0.109	–0.032	0.128	–0.010	–0.064	0.018
<i>P</i>	0.723	0.974	0.630	0.887	0.571	0.965	0.776	0.936
10–12 mm								
<i>r</i>	0.360	0.377	–0.015	0.142	–0.123	–0.105	–0.043	0.098
<i>P</i>	0.100	0.084	0.946	0.529	0.587	0.642	0.850	0.323
Total diameter								
<i>r</i>	0.360	0.351	0.008	0.145	0.047	–0.091	–0.082	–0.223
<i>P</i>	0.100	0.109	0.972	0.519	0.836	0.685	0.717	0.318
Center								
0–2 mm								
<i>r</i>	0.499	0.361	0.008	–0.002	–0.141	0.088	0.044	0.078
<i>P</i>	0.018	0.099	0.971	0.994	0.532	0.697	0.846	0.732
2–6 mm								
<i>r</i>	0.416	0.398	–0.008	0.027	–0.104	0.045	–0.046	0.105
<i>P</i>	0.054	0.066	0.971	0.906	0.645	0.843	0.838	0.643
6–10 mm								
<i>r</i>	0.113	–0.087	0.230	–0.166	0.249	0.056	0.029	–0.072
<i>P</i>	0.616	0.702	0.304	0.461	0.264	0.805	0.900	0.750
10–12 mm								
<i>r</i>	0.278	0.316	–0.175	0.259	–0.228	–0.084	0.021	–0.396
<i>P</i>	0.211	0.151	0.436	0.245	0.307	0.709	0.924	0.068
Total diameter								
<i>r</i>	0.241	0.402	–0.120	0.167	–0.184	–0.065	0.001	–0.405
<i>P</i>	0.540	0.064	0.596	0.458	0.413	0.774	0.995	0.062
Posterior 60 $\mu\text{m}$								
0–2 mm								
<i>r</i>	–0.202	0.399	0.053	0.010	0.237	0.056	–0.018	0.231
<i>P</i>	0.368	0.162	0.815	0.966	0.142	0.803	0.936	0.300
2–6 mm								
<i>r</i>	–0.219	0.258	0.100	0.001	0.207	0.148	0.031	0.242
<i>P</i>	0.327	0.099	0.658	0.998	0.516	0.512	0.890	0.277
6–10 mm								
<i>r</i>	–0.232	0.167	0.196	–0.244	0.027	0.072	0.066	0.063
<i>P</i>	0.300	0.366	0.382	0.274	0.921	0.749	0.769	0.782
10–12 mm								
<i>r</i>	0.370	0.527	–0.158	0.181	0.507	–0.046	0.046	–0.375
<i>P</i>	0.090	0.012	0.482	0.420	0.016	0.839	0.841	0.086
Total diameter								
<i>r</i>	0.041	0.211	0.045	–0.032	0.285	0.028	0.029	–0.036
<i>P</i>	0.856	0.345	0.843	0.888	0.198	0.901	0.897	0.875
Total thickness								
0–2 mm								
<i>r</i>	0.315	0.278	0.033	0.104	0.083	0.080	–0.027	0.163
<i>P</i>	0.153	0.209	0.882	0.645	0.713	0.723	0.905	0.468
2–6 mm								
<i>r</i>	0.289	0.283	0.083	0.063	0.131	0.040	–0.072	0.117
<i>P</i>	0.192	0.202	0.715	0.781	0.561	0.858	0.749	0.605
6–10 mm								
<i>r</i>	0.114	–0.033	0.123	–0.050	0.226	0.008	–0.023	0.017
<i>P</i>	0.612	0.885	0.587	0.826	0.312	0.972	0.917	0.941
10–12 mm								
<i>r</i>	0.350	0.335	–0.045	0.124	–0.138	–0.081	0.001	–0.058
<i>P</i>	0.110	0.127	0.843	0.584	0.539	0.719	0.998	0.677
Total diameter								
<i>r</i>	0.319	0.379	–0.042	0.153	0.053	–0.064	–0.025	–0.246
<i>P</i>	0.148	0.082	0.854	0.496	0.814	0.778	0.910	0.270

ALT, alanine aminotransferase; AST, aspartate aminotransferase; Cp, ceruloplasmin; GGT, gamma-glutamyl transferase; *r*, Spearman correlation coefficient.

Table 6. Relationship between the clinical and laboratory findings of subjects with Wilson disease and lens densitometry values

	Age	Duration of WD	Serum Cp	24-hour urinary copper excretion	Liver copper content	ALT	AST	GGT
Zone 1								
<i>r</i>	0.304	0.426	-0.148	0.158	0.178	0.148	-0.083	0.024
<i>P</i>	0.169	0.018	0.512	0.482	0.429	0.512	0.715	0.916
Zone 2								
<i>r</i>	0.153	0.151	-0.180	0.152	0.161	0.239	0.020	0.159
<i>P</i>	0.497	0.535	0.422	0.500	0.475	0.284	0.930	0.481
Zone 3								
<i>r</i>	0.318	0.259	-0.206	0.342	0.250	0.210	-0.011	0.018
<i>P</i>	0.150	0.244	0.358	0.120	0.262	0.349	0.962	0.937
Average								
<i>r</i>	0.224	0.121	-0.122	0.418	0.159	0.318	0.089	0.254
<i>P</i>	0.317	0.591	0.588	0.053	0.481	0.149	0.695	0.255
SD								
<i>r</i>	0.188	0.096	0.140	0.107	0.001	0.367	0.231	-0.109
<i>P</i>	0.402	0.670	0.535	0.636	0.996	0.093	0.300	0.628
Maximum								
<i>r</i>	0.267	0.096	0.003	0.196	0.345	0.321	0.136	-0.009
<i>P</i>	0.230	0.672	0.990	0.382	0.115	0.145	0.545	0.968
Lens thickness, mm								
<i>r</i>	0.170	0.149	0.051	0.168	0.181	0.169	-0.090	0.290
<i>P</i>	0.449	0.509	0.821	0.454	0.421	0.451	0.690	0.190

ALT, alanine aminotransferase; AST, aspartate aminotransferase; Cp, ceruloplasmin; GGT, gamma-glutamyl transferase; *r*, Spearman correlation coefficient; SD, standard deviation.

they are not “true” cataracts.<sup>21</sup> Tso and colleagues<sup>22</sup> studied eyes with sunflower cataracts via biopsy and reported that the granules were located mostly in the anterior lens capsule in the middle of lens, thus leaving the equatorial capsule relatively free of accumulation. We detected higher lens densitometry values in the central zone and in the mean values of the average measurements in children with WD but no sunflower cataracts than control eyes. We believe that, starting from the center, copper accumulation alters lens clarity, even when sunflower cataracts are not present on slit-lamp examination. We also found a significant correlation between lens densitometry at zone 1 and the duration of WD, suggesting that the cumulative effects of copper accumulation result in decreased lens clarity.

The current study is limited by the relatively low number of subjects. Other possible limitations are the lack of confocal microscopy and AS-OCT data, which could have been helpful in correlating our results, and the lack of corneal and lens densitometry measurements of children with KF rings and sunflower cataracts. The duration of WD was relatively short, because the study subjects were children. Also, because of the cross-sectional design of our study, we could not evaluate the effect of systemic treatment on densitometry measurements in the long term in our cohort. Nevertheless, this study provides the first evidence about corneal and lens clarity in pediatric WD patients.

## Literature Search

PubMed was searched, without date or language restriction, using the following terms: *Wilson disease AND chil-*

*dren, Kayser-Fleischer rings, sunflower cataracts, corneal densitometry, lens densitometry, and anterior segment imaging.*

## References

1. Thomas GR, Forbes JR, Roberts EA, Walshe JM, Cox DW. The Wilson disease gene: spectrum of mutations and their consequences. *Nat Genet* 1995;9:210-17.
2. Ala A, Walker AP, Ashkan K, Dooley JS, Schilsky ML. Wilson's disease. *Lancet* 2007;369:397-408.
3. Mak CM, Tam S, Fan ST, Liu CL, Lam CW. Wilson's disease: a patient undiagnosed for 18 years. *Hong Kong Med J* 2006;12:154-8.
4. Socha P, Janczyk W, Dhawan Y, et al. Wilson's disease in children: a position paper by the Hepatology Committee of the European Society for Paediatric Gastroenterology, Hepatology and Nutrition. *J Pediatr Gastroenterol Nutr* 2018;66:334-44.
5. Nicastro E, Ranucci G, Vajro P, Vegnente A, Iorio R. Re-evaluation of the diagnostic criteria for Wilson disease in children with mild liver disease. *Hepatology* 2010;52:1948-56.
6. Roberts EA, Schilsky ML, American Association for Study of Liver Diseases (AASLD). Diagnosis and treatment of Wilson disease: an update. *Hepatology* 2008;47:2089-111.
7. Merle U, Schaefer M, Ferenci P, Stremmel W. Clinical presentation, diagnosis and long-term outcome of Wilson's disease: a cohort study. *Gut* 2007;56:115-20.
8. Patil M, Sheth KA, Krishnamurthy AC, Devarbhavi H. A review and current perspective on Wilson disease. *J Clin Exp Hepatol* 2013;3:321-36.
9. Dobbs RE, Smith JP, Chen T, Knowles W, Hockwin O. Long-term follow-up of lens changes with Scheimpflug photography in diabetics. *Ophthalmology* 1987;94:881-90.
10. Sasaki H, Hockwin O, Kasuga T, Nagai K, Sakamoto Y, Sasaki K. An index for human lens transparency related to age and lens layer: comparison between normal volunteers and diabetic patients with still clear lenses. *Ophthalmic Res* 1999;31:93-103.
11. Weiner X, Baumeister M, Kohnen T, Bühren J. Repeatability of lens densitometry using Scheimpflug imaging. *J Cataract Refract Surg* 2014;40:756-63.

12. Otri AM, Fares U, Al-Aqaba MA, Dua HS. Corneal densitometry as an indicator of corneal health. *Ophthalmology* 2012;119:501-8.
13. Ferenci P, Caca K, Loudianos G, et al. Diagnosis and phenotypic classification of Wilson disease. *Liver Int* 2003;23:139-42.
14. Elflein HM, Hofherr T, Berisha-Ramadani F, et al. Measuring corneal clouding in patients suffering from mucopolysaccharidosis with the Pentacam densitometry programme. *Br J Ophthalmol* 2013;97:829-33.
15. Giacchino R, Marazzi MG, Barabino A, et al. Syndromic variability of Wilson's disease in children. Clinical study of 44 cases. *Ital J Gastroenterol Hepatol* 1997;29:155-61.
16. Belkin M, Zeimer R, Chajek T, Friedman G, Melamed E. Non-invasive quantitation of corneal copper in hepatolenticular degeneration (Wilson's disease). *Lancet* 1976;1:391-2.
17. Ceresara G, Fogagnolo P, Zuin M, Zatelli S, Bovet J, Rossetti L. Study of corneal copper deposits in Wilson's disease by in vivo confocal microscopy. *Ophthalmologica* 2014;231:147-52.
18. Sridhar M. Advantages of anterior segment optical coherence tomography evaluation of the Kayser-Fleischer ring in Wilson disease. *Cornea* 2017;36:343-6.
19. Telinius N, Ott P, Hjortdal J. Detection of Kayser-Fleischer ring using Scheimpflug imaging. *Acta Ophthalmologica* 2017;95:248-9.
20. Harry J, Tripathi R. Kayser-Fleischer ring. A pathological study. *Br J Ophthalmol* 1970;54:794-800.
21. Goyal V, Tripathi M. Sunflower cataract in Wilson's Disease. *J Neurol Neurosurg Psychiatry* 2000;69:133.
22. Tso MO, Fine BS, Thorpe HE. Kayser-Fleischer ring and associated cataract in Wilson's disease. *Am J Ophthalmol* 1975;79:479-88.